Journal of Innovative Optical Health Sciences
Vol. 5, No. 1 (2012) 1150010 (7 pages)

DOI: 10.1142/S1793545811500106

DESIGN AND FABRICATION OF A 20 MHz ANNULAR ARRAY FOR MEDICAL ULTRASOUND

ZHENHUA HU and JUE PENG*
Department of Biomedical Engineering
School of Medicine, Shenzhen University
Shenzhen, Guangdong 518060, China
**eureka_peng@yahoo.com.cn*
**erica@szu.edu.cn*

Accepted 18 October 2011
Published 20 December 2011

Most high frequency (>15 MHz) medical ultrasound systems are based on single element transducers mechanically scanned. These systems can provide images with excellent resolution. However, single element transducers are often limited by the fixed focal point and small depth of field. Annular arrays consisting of concentric rings of elements are focused electronically. These arrays are desirable to avoid the fixed focal point of the single element transducers and improve the depth of field. This paper reports the design, fabrication, and characterization of a 5-element equal-area annular array transducer. After electrical impedance matching, the average center frequency was 20 MHz and −6 dB bandwidths ranged from 34 to 42%. The ILs for the matched annuli ranged from 6.1 to 26.5 dB.

Keywords: High frequency phased array; medical ultrasonic; transducer.

1. Introduction

The field of high-frequency ultrasound (HFU) imaging, using frequencies above 15 MHz, is growing rapidly as transducer technologies are improving and the cost of high bandwidth electronic instrumentation is decreased. With increased ultrasound frequency, the spatial resolution can be improved, but at the same time the penetration depth of ultrasound waves into the tissue is decreased because of frequency-dependent attenuation. Therefore, high frequency imaging systems can be advantageously applied to small-size objects, such as near-surface areas (skin vessels), low-attenuation tissues (eyes), or small animals.[1] Most of the high frequency medical ultrasound systems are based on single element transducers mechanically scanned. These systems can provide images with excellent resolution. However, single element transducers are often limited by the fixed focal point and small depth of field. A linear or a phased array can use electronic delays to dynamic focusing and beam steering. However, fabricating these high arrays is very difficult. For example, a 50 MHz linear array requires an element spacing of 30 μm (and a phased array 15 μm) to avoid unwanted regions of constructive interference in the imaging systems called grating lobes.[2] A few researches have successfully developed linear arrays operating at ultrasound frequencies above 50 MHz.[3] Unfortunately, fabricating these high arrays is very challenging.

*Corresponding author.

Annular arrays are consisting of concentric rings of elements which were focused electronically. These arrays are desirable to avoid the fixed focal point of the single element transducers. Though annular arrays do not provide beam steering, they do allow for dynamic focusing along the axis. These devices also need significantly fewer elements than linear-sequenced arrays or linear-phased arrays, thus reducing the complexity of the electronics, more importantly, the axial symmetry of annular arrays lead to the formation of a high quality radiation pattern. However, like single element transducers, annular arrays unfortunately rely upon mechanical scan to form an image.

This paper discusses the design and fabrication of a high-frequency, annular-array transducer for application in medical imaging. An empirical formula was used to guide the design of a 20 MHz, 5.5-mm-diameter, 5-element annular array.[4] Individual elements were created by laser dicing and conventional cable soldering used for interconnection. Finally, test of the acoustic and electrical properties for annular array.

2. Design and Fabrication

2.1. *Annular array design*

The annular arrays can be divided into an equal-width design and an equal-area design. The equal-width annular array is easy to design and fabricate. However, this structure no longer has equal impedance and phase shift which leads to the complex driving and receiving circuits.[5] The equal-area array is consisting of concentric rings of equal-area elements. So, the equal-area constraints achieve approximately same electrical impedance which is ideal for impedance matching. More importantly, the phase shift across each element form signals on the axis of the array which will be identical for all the array elements. However, the widths of outer elements are decreased to maintain the equal-area condition, the width of the outermost element eventually becomes comparable to its thickness, resulting in the unwanted lateral mode coupling into the operating bandwidth of transducer. In this paper we design an equal-area annular array that is shown in Fig. 1. The diameter of the array will be given by[4]

$$D = \sqrt{8RN\gamma}, \tag{1}$$

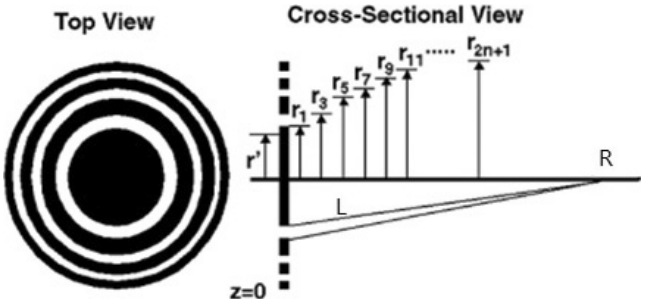

Fig. 1. Top/side view of an equal-area annular array.

where D is the diameter of the array, N is the number of elements, R is the focal distance, γ is the path difference, which is defined by subtracting the focal distance (R) from the distance between focal point and the outer edge of the array (L).

2.2. *Annular array fabrication*

The PZT-5H material is an ideal substrate for high-frequency transducers because of its high dielectric constant and high sensitivity. Several researchers have reported the development of high-frequency annular arrays using PZT-5H substrate.[4] For high-frequency devices, mechanical cutting is difficult. However, laser micromachining has been used successfully to fabricate 40−50 MHz annular array.[6] We fabricated the array by a commercial laser micromachining system which used an ultraviolet laser operating at 355 nm. An annular transducer array after lasing-cutting is shown in Fig. 2. As on the negative side of the PZT-5H without a layer of photoresist, during the laser-cutting process the resulting plasma debris is left in the electrode surface.[6]

First, we moved the annular array sample onto a glass slide. The slide was used as a carrier in all subsequent processing so that handling the fragile substrate was avoided. Second, the sample electrode surface was cleaned using acetone. Interconnection between the coaxial cables and transducer was completed with 90 μm wires which soldered directly the elements. Next, a brass housing was placed around the array, then partially filled using an insulating epoxy (Epotek-301) loaded tungsten powder to create an acoustically lossy backing material. After curing, the annular array transducer was released from the glass slide. The ground connections were soldered to the brass housing. Finally, the annular array was poled under DC voltage at room temperature in air.

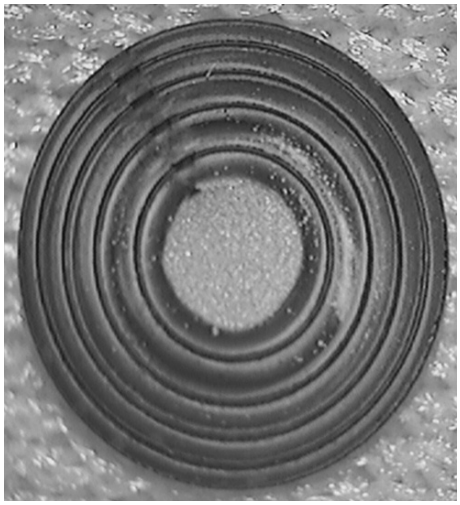

Fig. 2. Annular transducer array after lasing-cutting.

The piezoelectric transducer elements usually have very large acoustic impedance (>30 Mrayls) while the bodies to be imaged have very low acoustic impedance (<1.6 Mrayls), the acoustic energy transmission efficiency is rather low. The acoustic mismatching problem can be resolved using 1 or 2 quarter-wavelength matching layers, and the required matching layer materials usually should have acoustic impedance in the range of 3 to 14 Mrayls.[7] The impedance and sound velocity of the parylene-C is near 2.7 Mrayls and 2.2 km/s, respectively. The parylene-C also offers lower acoustic attenuation and easy application with thickness ranging from sub-micron to several microns. This material is also relatively inert and stable which should make it ideal for matching layer applications.[8] So, a layer of vapor deposited parylene-C with a thickness of 30 μm was coated on the annular array transducer surface as an acoustic matching layer, which is used to improve ultrasonic energy transmission between the piezoelectric material and the load medium.

3. Results and Discussion

3.1. *Testing*

3.1.1. *Pulse/Echo*

The transducers were first characterized by examining their pulse echo response using a stainless steel-plate target positioned 4 mm from the transducer. The transducer was placed in a small container of deionized water with a 3 cm thick stainless steel plate at its bottom. A pulser/receiver (5900PR, Olympus) was used to excite the transducer and receive the echo waveform. The pulses were recorded using a high-speed digital oscilloscope and the spectra were calculated in software. From the measured frequency spectra of the transducers, the following parameters of the transducer can be calculated by[9]

$$F_c = \frac{F_l + F_u}{2}, \tag{2}$$

$$BW_{-6dB} = \frac{F_u - F_l}{F_c} \times 100\%, \tag{3}$$

where F_c is the center frequency, F_u and F_l are the frequencies at which the magnitude of the amplitude in the spectrum is 50% (−6 dB) of the maximum.

3.1.2. *Two-way insertion loss*

The two-way insertion loss was measured by a function generator (AFG-3102, Tektronix) with 50 Ω output impedance. A tone burst of a 20-cycle sine wave with an amplitude of 1 V was generated over the array's pass-band, as measured by the oscilloscope with 50 Ω coupling. The voltage amplitude of the received echo was measured by the oscilloscope with 1 MΩ coupling. Then, the insertion loss was calculated by

$$\mathrm{I_L[dB]} = 20\mathrm{lg}\left(\frac{\mathrm{Vpp-emitted}}{\mathrm{Vpp-echo}}\right), \tag{4}$$

where V_{pp}-echo is the amplitude of echo signal, V_{pp}-emitted is the amplitude of excitation signal.

3.1.3. *Complex impedance*

The complex impedance of each annulus was measured with a precision impedance-analyzer (4294A, Agilent). The transducer was placed in the deionized water. Impedance measurements were made of each annulus in order to determine the most efficient electrical matching.

3.2. *Unmatched transducer*

Table 1 summarizes the values for the center frequency, and −6 dB bandwidth for all five annuli

Table 1. Summary of unmatched transducer performance.

Ring	F_c (MHz)	$BW_{-6\,dB}$ (%)	F_{IL} (MHz)	IL (dB)
1	20.7	25.9	21.0	10.6
2	19.3	43.1	22.0	21.2
3	19.2	50.5	20.3	34.2
4	19.9	44.7	22.0	35.7
5	19.8	46.9	20.2	36.8

without impedance matching. Table 1 also shows the results for minimum insertion loss and the frequency at which it occurred. Diffraction compensation and attenuation compensation are not considered, the central annulus's insertion loss achieved 10.6 dB, but the −6 dB bandwidth is lower than the other four rings.

Figure 3(a) shows the time-domain waveform acquired for Ring 3. The frequency-domain signal for Ring 3 is shown in Fig. 3(b). The center frequency (F_c) is 19.2 MHz and the −6 dB fractional bandwidth is 50.5%.

3.3. *Matched transducer*

The complex impedance of ring 3 was measurement with a 4294A impedance analyzer, save the impedance data as s1p format, import the s1p data to Genesys RF and Microwave Design Software (Agilent) for impedance matching. Genesys Matching Network synthesis quickly enables a circuit designer to create narrow or broadband matching networks between any two frequency varying impedances. The LC-Tee network was chosen for ring 3, and the schematic is shown in Fig. 4. Port 1 represents the input impedance of 50 Ω, port 2 is the impedance of ring 3, and $L1$ and $C1$ are inductance and capacitance of the matching circuit, respectively. With the impedance matching accomplished, we repeated the impedance measurements.

The impedance experimental results and Genesys model prediction for ring 3 are shown in Fig. 5(a). The unmatched element impedance is too low, resulting in electrical mismatch. The matched element impedance closes to 50 Ω, which has improved. The variation in impedances between the simulation and the experimental measurement was likely caused by two factors. First, the actual values and the simulation component values are different; second, in the Genesys simulation processing, wires, parasitic capacitances are not considered. The scattering parameter in the experimental result of Fig. 5(b) compare favorably to the predictions of the Genesys matching model. The unmatched element's minimum scattering parameter is only −4 dB, it shows that in the process of power transmission most of the energy is lost. Although, the experimental scattering parameter (−30 dB) is bigger than the simulation scattering parameter (−40 dB), the matching networks effectively reduce the scattering energy, improving the efficiency of power transmission.

The equal-area annular array constraints achieve approximately same electrical impedance,

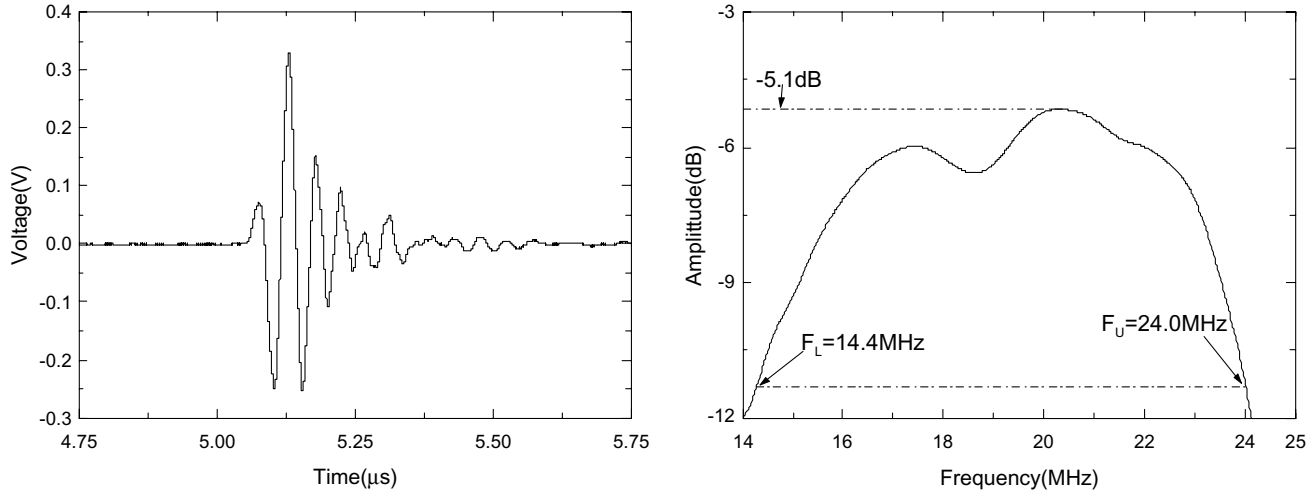

(a) (b)

Fig. 3. The pulse-echo response for No. 3 with no electrical matching. (a) Time-domain signal, (b) frequency-domain signal.

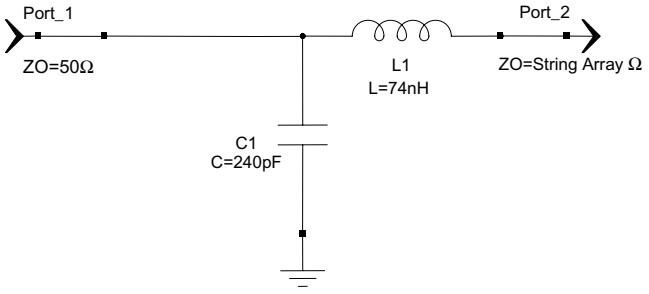

Fig. 4. The matching network for ring 3.

for simplicity, all of the array elements used the same matching network. With the impedance matching accomplished, we repeated the pulse/echo and IL measurements. The pulse/echo signal for ring 3 (matched) is shown in Fig. 6. Figure 6(a) shows the time-domain signal with electrical matching for ring 3, the echo amplitude compared to unmatched amplitude has improved. The peak voltage is 1.4 V; the corresponding frequency-domain signal with electrical matching for ring

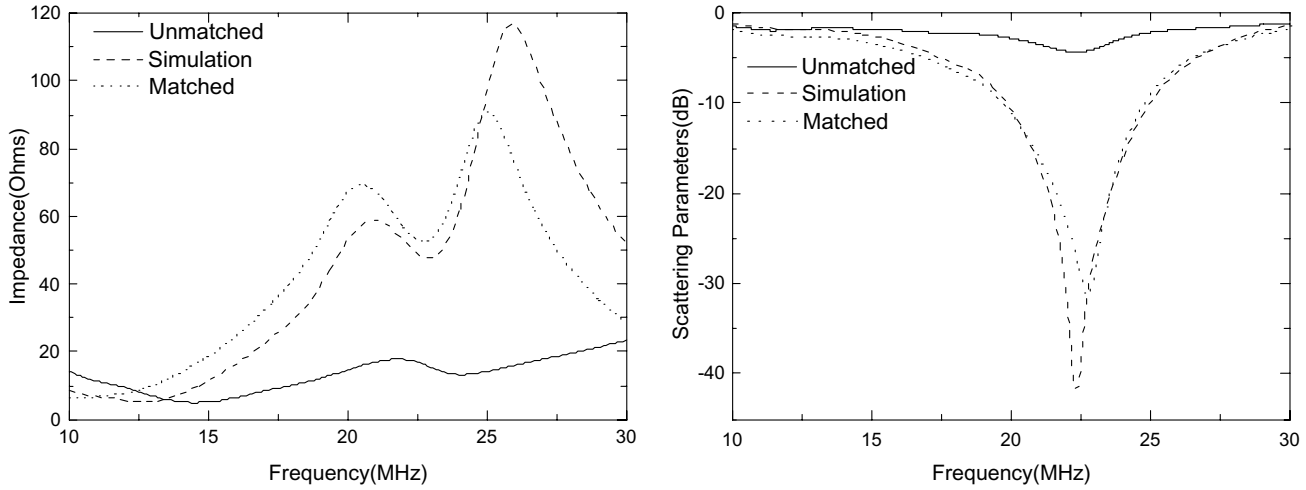

(a) (b)

Fig. 5. Comparison of simulation to experimental measurements for No. 3. (a) Impedance performances, (b) scattering parameters.

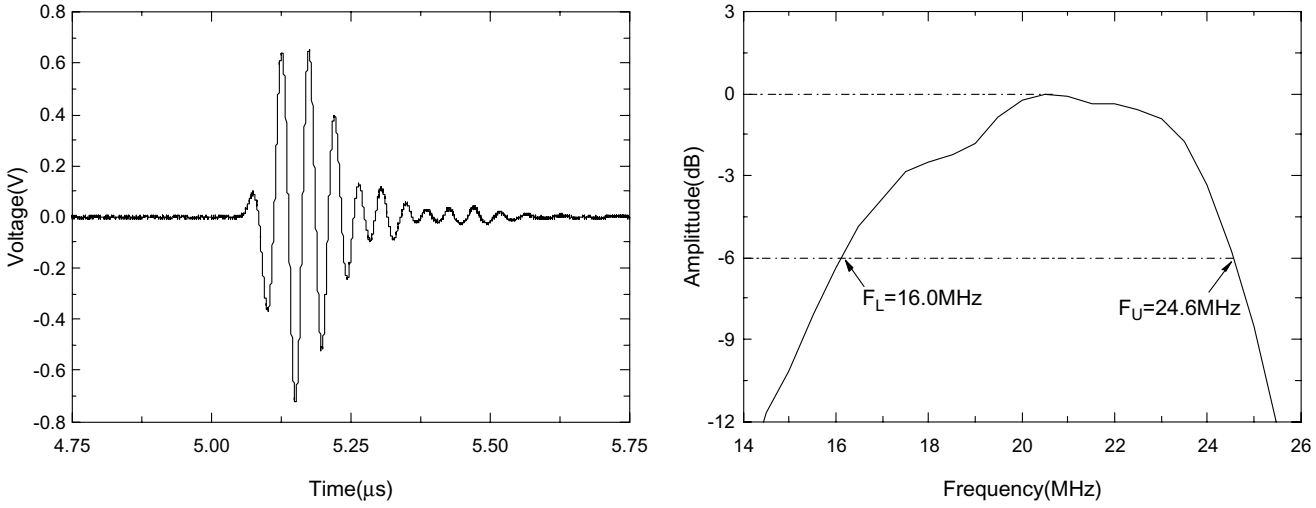

(a) (b)

Fig. 6. The pulse-echo response for No. 3 with electrical matching. (a) Time-domain signal, (b) frequency-domain signal.

3 is shown in Fig. 6(b), an upward shift in the center frequency, the values of the peak spectral amplitude increased by 5 dB, relative to the unmatched case.

The values of the center frequency, −6 dB bandwidth, the results for minimum insertion loss and the frequency at which it occurred for all five annuli are summarized in Table 2. Comparing these values to the unmatched case, it can be seen that the increase in pulse/echo sensitivity has been achieved at the cost of reduced bandwidth. The insertion loss for the annular array was significantly lower than what was reported fabricated previously by other groups design.[4–6]

The two-way radiation pattern was simulated using a software analysis package developed by Weidlinger Associates (PZFlex, Los Altos, CA). PZFlex uses a time-domain, finite-element algorithm, which is suited for the transient nature of pulsed ultrasound transducers.[10] Figure 7 shows the two-way radiation pattern that was simulated.

Table 2. Summary of matched transducer performance.

Ring	F_c (MHz)	$BW_{-6\,dB}$ (%)	F_{IL} (MHz)	IL (dB)
1	20.5	34.1	20.0	6.1
2	20.5	39.2	21.5	14.8
3	20.3	42.0	20.5	21.6
4	20.5	41.8	21.5	24.1
5	20.8	39.0	21.0	26.5

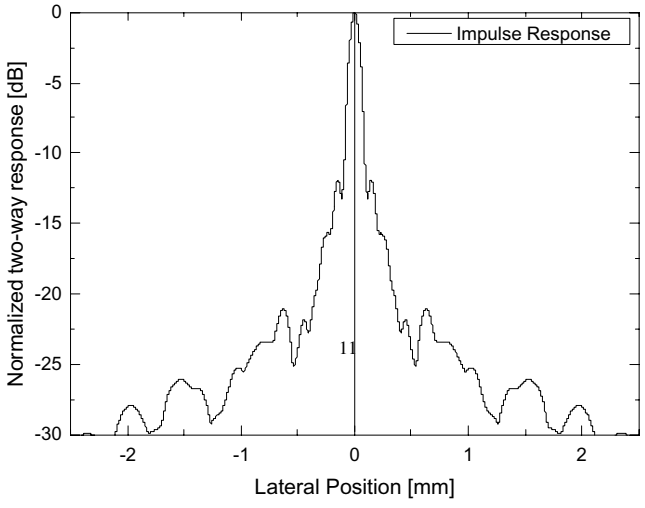

Fig. 7. Theoretical (impulse response method) radiation pattern for 5-element annular array with a focal distance of 3 mm.

The pedestal lobe is higher than the convention annular arrays, because of the high path difference. However, the width of the main beam is lower than the conventional 20 MHz transducers, which improves the lateral resolution (LR). In addition, wide bandwidth is also achieved leading to a good axial resolution. However, the experimental two-way radiation patterns and resolutions are still in preparation.

4. Summary and Conclusion

In this study, we reported the design and fabrication of a 5-element, equal-area annular array transducer, which has the advantage of lower insertion loss over previously reported annular arrays designs. After electrical impedance matching, the average center frequency was 20 MHz and −6 dB bandwidths ranged from 34 to 42%. The ILs for the matched annuli ranged from 6.1 to 26.5 dB. In the calculation of insertion loss, the diffraction loss factor was not considered, so the insertion loss for the outside array elements increases. The average insertion loss for the annular array (20 MHz:18.6 dB) was significantly lower than what was reported for the PZT-based annular array (44 MHz:38.6 dB) fabricated previously by Snook's group using the same design.[6] In the future, to verify the accuracy of simulation results, we plan to measure the two-way radiation patterns and lateral resolution.

Acknowledgments

This work was supported by the National Natural Science Foundation of China (Grant Nos. 10904093 and 61031003), the Science and Technology Grant Scheme funds from Shenzhen Government (No. 08CXY-23).

References

1. M. Vogt, J. Opretzka, C. Perrey, H. Ermert, "Ultrasonic microscanning," *Proc. IME H: J. Eng. Med.* **224**, 225–240 (2010).
2. K. K. Shung, M. Zippuro, "Ultrasonic transducers and arrays," *Eng. Med. Biol. Mag.* **15**, 20–30 (1996).
3. D. W. Wu, Q. Zhou, X. Geng, C. G. Liu, F. Djuth, K. K. Shung, "Very high frequency (beyond 100

MHz) PZT kerfless linear arrays," *IEEE Trans. Ultrason. Ferroelectrics Freq. Contr.* **56**, 2304−2310 (2009).
4. J. A. Brown, C. E. M. Demore, G. R. Lockwood, "Design and fabrication of annular arrays for high-frequency ultrasound," *IEEE Trans. Ultrason. Ferroelectrics Freq. Contr.* **51**, 1010−1017 (2004).
5. Y. Qian, N. Harris, "Development of high frequency annular array with a novel structure for medical imaging," *Procedia Eng.* **5**, 1276−1279 (2010).
6. K. A. Snook, H. Chang-Hong, T. R. Shrout, K. K. Shung, "High-frequency ultrasound annular-array imaging. Part I: Array design and fabrication," *IEEE Trans. Ultrason. Ferroelectrics Freq. Contr.* **53**, 300−308 (2006).
7. Q. Zhou, J. Cha, Y. Huang, R. Zhang, W. Cao, K. K. Shung, "Alumina/epoxy nanocomposite matching layers for high-frequency ultrasound transducer application," *IEEE Trans. Ultrason. Ferroelectrics Freq. Contr.* **56**, 213−219 (2009).
8. B. Hadimioglu, B. Khuri-Yakub, "Polymer films as acoustic matching layers," *Ultrasonic Symposium*, Vol. 3, pp. 1337−1340, IEEE (1990).
9. J. Peng, S. Lau, C. Chao, J. Dai, H. L. W. Chan, H. Luo, B. Zhu, Q. Zhou, K. Shung, "PMN-PT single crystal thick films on silicon substrate for high-frequency micromachined ultrasonic transducers," *Appl. Phys. A: Mater. Sci. Process.* **98**, 233−237 (2010).
10. G. Wojcik, D. Vaughan, N. Abboud, J. Mould Jr, "Electromechanical modeling using explicit time-domain finite elements," *Ultrasonic Symposium*, Vol. 1102, pp. 1107−1112, IEEE (1993).